Biosynthesis and characterization of CuO nanoparticles from plant of Adenathera pavonina linn bark and leaves.

TAIWO FELICIA OWOEYE (felicia.owoeye@covenantuniversity.edu.ng)
Covenant University https://orcid.org/0000-0002-2055-3919
Kehinde Deborah Akinlabu
Moses Emetere
Yinka John ADEBOYE

Research Article

Keywords: Adenathera pavonina linn, plant extract, copper nanoparticles, biosynthesis, characterization

Posted Date: February 25th, 2022

DOI: https://doi.org/10.21203/rs.3.rs-1366337/v1

Abstract

Copper, a naturally occurring element, has medicinal potential and has recently gained in the textile industry. This paper seeks to chart the way forward on the commercial production of copper nanoparticles (Cu-NPs) for textile industry. The leaves and bark of Adenathera pavonina linn were used to synthesize copper nanoparticles (Cu-NPs) which are utilized in a range of applications as heterogeneous catalysts in textile industry. Copper nanoparticles were created using a chemical and natural method (Leaf extraction). In the absence of any reducing or stabilizing agents, the assynthesized samples were submitted to a range of analytical techniques in order to learn more about the physical properties of the materials. The radius of the Cu-NP from leave extract ranged from 56 nm – 89 μm with copper, carbon, and oxygen having a composition of 73.31%, 6.40% and 20.29% respectively. Likewise, the radius of Cu-NP from bark extract ranged from 56 nm – 293 μm with copper, oxygen, carbon, silicon, manganese, and aluminum having a composition of 65%, 24%, 1.22%, 4.20%, 3.10%, and 2.12% respectively. The impurities are largely from soil which the plant takes its nutrient. Carbon was found in both extract as it is expected in organic compounds in plants. The crystalline characterization shows that their exist a significant composition of Cu (I) species in both Cu-NP from the extracts that makes it highly relevant to the catalytic procedure in the textile industries. Each feature of the planes shows the copper atom represented as Cu-1 and Cu-2. Since Adenathera pavonina linn is in abundant in the tropics, its sustainability and low-cost production and processing are highly desired for textile industries.

1. Introduction

Microbes, plant extracts, and other natural bio-materials have been utilized to manufacture metal nanoparticles, according to reports [1–2]. Scientists have shown over time that his green synthesis approach is environmentally friendly for the production metallic nanoparticles which has found wide application in medicine [3] and solar cell applications [4]. One of the advantages of biosynthesis approach is its ability to produce different sizes and shapes of metallic nanoparticles for different applications [5]. Plant extracts are a better way to produce nanoparticles since they are chemical-free and also serve as natural capping agents. Plant extracts reduce synthesis expenses by removing the costs of isolation and culture medium improvement, as compared to microorganism synthesis. As lowering agents, biomolecules have been revealed to have a significant advantage over their protective counterparts [6–10].

Copper inhibits a wide range of bacterial types and pathogens commonly encountered in medical and industrial settings. Several researchers had worked on copper for several reasons. Letchumanan et al. [5] examined an indepth review of literatures to determine the potential of developing plant-based Cu/CuO nanoparticles (NPs) as a therapeutic agent for various diseases. They noted that the extraction of the copper NPs was from mainly the leaves of plants which have different properties due to the diversity in metabolite composition. Aside, the metabolite composition of the plant extracts the antimicrobial activity was investigated to ascertain if it were adequate for medicinal application. Prabhu et al. [11] revealed that the copper NPs are highly antibacterial against Escherichia coli and Staphylococcus aureus. Aside the

plants that was used i.e., Garcinia mangostana leaf extract, the size and shape of the nanoparticles seems to have significant effect on shape and sizes of the NPs. Navid et al. [12] considered a wholistic approach towards copper NPs production for medicinal application i.e., using Achillea millefolium leaf extracts. Four parameters were considered to enhance production i.e., catalyst, temperature, time of reaction and synthetic routes. Despite, the optimization of the Cu NPs, it was reported the Cu NPs had both anti-fungal and anti-bacterial properties as they were screened against Staphylococcus aureus, M. tuberculosis, E. coli, K. pneumoniae, P. mirabili, C. diphtheriae and S. pyogenes bacteria's and G. albicans, A. flavus, M. canis and G. glabrata fungus with an excellent which largely depends on the concentration of the NPs. Cu NPs have been reported to have high potential to rupture the fungi or bacteria's cell wall [13]. Prema and Thangapandiyan [14] reported that the cell-wall rupturing is largely enabled by large surface area, which NPs to have a better contact with the fungi or bacterial cell wall.

In present time, the use of microbes i.e., extract of green alga Botryococcus braunii for the synthesis of copper nanoparticles have been documented in Ref [14]. Despite its high anti-fungal and anti-bacterial properties which was successfully tested against two Gram-negative bacterial strains Pseudomonas aeruginosa (MTCC 441) and Escherichia coli (MTCC 442), two Gram-positive bacterial strains Klebsiella pneumoniae (MTCC 109) and Staphylococcus aureus (MTCC 96), and a fungal strain Fusarium oxysporum (MTCC 2087), its ingestion into the human body is somewhat questionable because of the synthesis route that requires 1 mM aqueous copper acetate. In same vein, Bukhari et al. [15] worked on a notable microbe found in marine environment i.e., Streptomyces sp. Despite its high anti-microbial potentials against Enterococcus faecalis ATCC 29212, Salmonella typhimurium ATCC 14028, Pseudomonas aeruginosa ATCC 9027, Escherichia coli ATCC 8939, fungi (Rhizoctonia solani, Fusarium solani, and Aspergillus niger), and yeast (Candida albicans ATCC 10237), the use of 5 mM of copper sulfate ($CuSO_4$) is worrisome for actual application to human.

Due to the edibility issues surrounding copper NPs, the application focus has grown into the broad field of calatalyst which has been found to have wide application to the engineering of materials. Dipali et al. [16] has clearly shown that copper NPs are used for different catalytic processes such as electrocatalysis, photocatalysis, and gas-phase catalysis. The catalytic process has found huge application to cotton textiles [17]. Nabil et al. [18] used the catalytic process to coat polyester fabric (PF) via the facile method which resulted to the generation of new functional sites at the PF surface via catalytic reduction of 4-nitrophenol (4-NP) to 4-aminophenol (4-AP). Golnaz et al. [19] used the copper NPs as a catalyst with new functional sites i.e., using different ligands including (3-Aminopropyl) triethoxysilane (APTS), oleic acid (OA) and polyacrylic acid (PAA) to enhance the technology for electronic textiles. It was reported that the overall best performing copper NPs catalyst was CuNP-PAA which had Cu (I) species whose amount about 1.7%. The efficacy of the catalyst depends on size and dispersal ability of Cu (I) present in the catalyst. Based on this vital discovery, the focus of this paper is to synthesize a high content Cu (I) in a copper NPs for textile application.

2. Materials And Methods

Only analytical reagent-grade materials and solvents were used in the synthesis. The samples were prepared with fresh distilled water throughout the operation. The bark and leave samples of Adenanthera pavonina linn were collected without damaging the parent plant. Adenanthera pavonina linn are very common in the tropics. The leaves of Adenanthera pavonina linn were thoroughly washed in distilled water severally to remove dust depositions. These leaves were dried and crushed to make powder. The extract was then filtered through Whatman's No. 1 filter paper. The filtrate was collected in a clean and dry container and stored for later use without being purified or analyzed. Two filtrate containers were obtained i.e., the leave extract container and the bark extract container.

The preserved filtrate was further processed by dissolving 0.1M Copper Sulphate in 100 ml distilled water, then adding 30ml extract dropwise into the solution. The samples were stirred for homogeneity using magnetic stirer for 4 hours. After stirring, it is believed that a complex functional will be formed which was further centrifuged at 7000 rpm for 15 minutes to collect it. After that, the centrifuge substrates were cleaned with distilled water before being centrifuged at 5000 rpm for another 10 minutes. The separated complex substrate was dried for 8 hours at 40°C before being calcined at 450°C in a muffle furnace for three hours to burn off any residual organic moiety, resulting in biosynthesized copper nanoparticles. Also, the calcination is to remove excess oxides in the sample. The resulting compound was characterized i.e., the microstructural and morphology of the copper nanoparticles was characterized by scanning electron microscope (SEM) analysis; the X-ray diffraction (XRD) spectrum was used to characterize the crystalline nature of the compound; and Fourier transform infrared (FTIR) analysis was used to determine the functional groups; and EDS analyses was used to examine the elemental composition of the copper nanoparticles.

3. Results And Discussion

The microstructure and morphology of the samples was characterized using the scanning electron microscope (SEM) as presented in Figs. 1 & 2. The parameters used for the characterization is as follows: magnification of 8000, pressure of 70 Pa, high voltage system of 15 kV, horizontal field width (HFW) OF 120 µm, and working distance (WD) of 10 mm. Individual copper oxide particles are agglomerated in the SEM pictures. A closer examination reveals the presence of multiple nanoparticle aggregates in the agglomerated mass. Particles appear to be agglomerated in the in Figs. 1 and 2 with the copper nanoparticle (Cu-NP) in leave extract having tinier particles than the Cu-NP in bark extract. The Cu-NP from bark extract have higher porosity than the Cu-NP from leave extract. Porosity is vital for catalytic processes [20]. The colony formed in both images shows the presence of binding functional group whose component may be explicit in the EDS characterization. The particulate size and distribution are presented in Fig. 3 below. The radius of the Cu-NP from leave extract ranged from 56 nm – 89 µm (Fig. 3b) while the Cu-NP from bark extract ranged from 56 nm – 293 µm (Fig. 3b). The Cu-NP from leave extract was seen to be compact while the Cu-NP from bark extract shows the presence of six main clogs. Hence, considering the application of the Cu-NP from both extract,

The EDX analysis reveals the elemental composition in both extracts. Figure 4 shows the elemental composition in the Cu-NP from bark extract. The highest element in the intensity are (Copper (Cu)—-65.0%, Oxygen(O)—-24.0%,).There are other element observed in the EDX spectrum(Carbon(C)—-1.22%,Silicon (S)—4.20,(Mn)—3.10,Aluminium (Al)—2.12 (Fig. 4). This may be the result of residual element originally present in the plant extract. The highest element in the intensity are (Copper (Cu)—-73.31%, Oxygen(O)—-20.29%,).

Comparatively, the bark has added impurities of manganese, silicon, and aluminum which may be absorbed from the soil. Carbon was found in both extract as it is expected in organic compounds in plants. The composition of Cu (I) species in both Cu-NP from the extracts is very high which gives credence to its applicability for catalytic procedure in the textile industries.

The XRD measurement was further carried out using the XRD Rigaku D/Max-IIIC model with generator tension and current given as 40 kV and 20 mA respectively. The scanning angle ranges from 32-73^{o}. Under a continuous scan technique under a maximum intensity of 1400cps, thirteen peaks were discovered but only eight was identified as presented in Fig. 6 below. The unidentified peaks are inherent impurity associated the plant constituents in the synthesis of the nanoparticles. The polycrystalline nanoparticles material was seen to have oxides between identified element such as copper, silicon, manganese, carbon, and aluminum. The crystalline arrangement is unique with extensive crystal growth from index surfaces of a cubic crystal system. For example, FWHM and d-spacing of planes (111) are 0.02 and 3.35 respectively while that of plane $(\bar{1}11)$ is 0.03 and 3.25 respectively depicts that the crystalline growth profiles is from face-centered cubic aluminum. Unlike the extensive growth in the first identified cubic crystal system, the second cubic crystal system had intercalated crystals (Takeuchi et al., 2017) as observed in planes (202) and $(\bar{2}02)$. From literature, the intercalated face-centered cubic system was identified as copper [21]. The other crystal planes were associated to the silicon, manganese, and carbon nanoparticles whose FWHM was > 0.1 and d-spacing < 2.5.

The XRD measurement parameter was same as Fig. 2. The scanning angle ranged from 10-70^{o}. Under a continuous scan technique under a maximum intensity of 300cps, nine peaks were discovered but only seven was identified as presented in Fig. 3 below. The two highest peaks had same plane i.e., $(\bar{1}11)$ but different FWHM and d-spacing. The first $(\bar{1}11)$ plane had FWHM and d-spacing of 0.028 and 3.53 respectively while the second $(\bar{1}11)$ plane had FWHM and d-spacing of 0.16 and 3.653. Each feature of the planes shows the copper atom represented as Cu-1 and Cu-2. Low Miller-index copper surfaces break up into nanoclusters in the presence of reactant gases. The unidentified peaks are inherent impurity associated the plant constituents in the synthesis of the nanoparticles. More so, the crystallographic features of the nanoparticles shows that the a-b axes represents where the crystal growth is significant.

The functional group analysis of Cu-NP from barkextract is presented in Fig. 7 below. The functional group has its orientation from Adenanthera pavonina bark extracts and Copper sulphate salt. Table 1

shows the summary of the analysis. Figure 7 shows the FTIR spectrum of the Adenanthera pavonina linn leave using bio-synthesized method, which involves the use of Adenanthera pavonina leaf extracts and Copper Sulphate salt. Table 2 shows the summary of the analysis. Comparatively, the functional group in both leave and bark extract clearly differs because its different properties are largely due to the diversity in its metabolite composition.

Table 1
FTIR spectra of Adenathera pavonina linn bark

FREQUENCY (cm^{-1})	ASSIGNMENT	POSSIBLE NUTRIENT	REFERENCES
3367.0	Aliphatic Primary amine,NH Stretch,Normal	Primary amine	[22]
2159.0	Thiocyanate (SCN)		[22]
1635.56	Organic nitrate (C-C Stretch of phenyl)	Protein amide 1	[22]
1411.0	Vinylidene C-H in plane bend	Organic ions,Olefinic (alkene)	[22]
1032.09	Cyclohexane ring vibrations Methylene (CH_2) Primary amine,C-N Stretch	Primary amino	[22]
506.00	Aliphatic Iodo compounds,Polysulfides S-S Stretch		[22]

Table 2
FTIR spectra of Adenathera pavonina linn leaves

FREQUENCY (cm^{-1})	ASSIGNMENT	POSSIBLE NUTRIENT	REFERENCES
3487.0	Heterocyclic amine N-H Stretch	Secondary amino	[22]
2350.0	N-H Component	Amino-related component	[22]
1647.0	Alkenyl C = C Stretch	Olefinic	[22]
1082.0	Primary amine,CN Stretch	Primary amine	[22]
798.86	Aliphatic Chloro compounds,C-Cl Stretch	Aliphatic Organohalogen compound	[22]
459.0	Aryl disulfides (S-S)Stretch		[22]

Conclusion

Adenanthera Pavonina leaf and bark plant was investigated extensively for the preparation of Copper nanoparticles to ascertain its relevance to the textile industries. The microstructural examination of Adenanthera Pavonina leaf and bark showed that the radius of the Cu-NP from leave extract ranged from 56 nm – 89 μm with copper, carbon, and oxygen having a composition of 73.31%, 6.40% and 20.29% respectively. Likewise the radius of Cu-NP from bark extract ranged from 56 nm – 293 μm with copper, oxygen, carbon, silicon, manganese, and aluminum having a composition of 65%, 24%, 1.22%, 4.20%, 3.10%, and 2.12% respectively. The result looks promising for commercial production of Cu-NP from Adenanthera Pavonina as the size, porosity, and Cu(1) and Cu(2) content are essential parameters that underscore the viability of the Cu-NP.

The crystalline characterization of the Cu-NP from Adenanthera Pavonina leaf and bark also shows that their exist a significant composition of Cu (1) and Cu (2) species in both Cu-NP from the extracts that makes it highly relevant to the catalytic procedure in the textile industries. Besides the textile industry, industries that needs photocatalyst at reduced cost of production may find this product handy. This work has, therefore, demonstrated the conversion of agricultural waste to wealth as discarded Adenanthera Pavonina biomass after harvest has found usefulness. The production process is cost-efficient, eco-friendly, and sustainable because the plant is very common in the tropics.

Declarations

Conflict of Interest

The authors declare no conflict of interest

References

1. S. Saif, A. Tahir, Y. Chen, Green synthesis of iron nanoparticles and their environmental applications and implications. Nanomaterials **6**, 209 (2016)
2. J. Thanuja, G. Nagaraju, H.R. Naika, Biosynthesis of Cu4O3 nanoparticles using Razma seeds: Application to antibacterial and cytotoxicity activities. SN Appl. Sci. **1**, 1–12 (2019)
3. H.W. Zhao, H.T. Su, A. Ahmeda, Y.Q. Sun, Z.Y. Li, M.M. Zangeneh, M. Nowrozi, A. Zangeneh, R. Moradi, Biosynthesis of copper nanoparticles using Allium eriophyllum Boiss leaf aqueous extract; characterization and analysis of their antimicrobial and cutaneous wound-healing potentials. Appl. Organomet. Chem. 2020
4. M.E. Emetere, T. Gabe-Oji, B.M. Durodola, Spectral filtering experimentation on Photovoltaic cells using novel bio-filter made from copper coated hibiscus-ethanol extract. Int. J. Electr. Comput. Eng. **10**, 3819 (2020)
5. D. Letchumanan, S.P.M. Sok, S. Ibrahim, N.H. Nagoor, N.M. Arshad. Plant-Based Biosynthesis of Copper/Copper Oxide Nanoparticles: An Update on Their Applications in Biomedicine, Mechanisms,

and Toxicity. Biomolecules. 2021 Apr 12;11(4):564. doi: 10.3390/biom11040564. PMID: 33921379; PMCID: PMC8069291

6. V. Bansal, D. Rautaray, A. Bharde, K. Ahire, A. Sanyal, A. Ahmad, M. Sastry
7. Fungus-mediated biosynthesis of silica and titania particles P. Mukherjee, A. Ahmad, D. Mandal, S. Senapati, S.R. Sainkar, M.I. Khan, R. Parishcha, P.V. Ajay, M. Alam, R. Kumar, M. Sastry Fungus-mediated synthesis of silver nanoparticles and their immobilization in the mycelia matrix: a novel biological approach to nanoparticle synthesisNano Lett., 1 (2001), pp. 515–519
8. N. Durán, P.D. Marcato, S. De, I.H. Gabriel, O.L. Alves, E. Esposito, Antibacterial effect of silver nanoparticles produced by fungal process on textile fabrics and their effluent treatment. J. Biomed. Nanotechnol **3**, 203–208 (2007)
9. A. Bharde, D. Rautaray, V. Bansal, A. Ahmad, I. Sarkar, S.M. Yusuf, M. Sanyal, M. Sastry (2006), Extracellular biosynthesis of magnetite using fungi Small, 2: 135–141
10. S.P. Chandran, M. Chaudhary, R. Pasricha, A. Ahmad, M. Sastry, Synthesis of gold nanotriangles and silver nanoparticles using Aloe vera plant extract Biotechnol. Prog. **22**, 577–583 (2006)
11. Y.T. Prabhu, V.K. Rao, V.S. Sai, T. Pavani, A facile biosynthesis of copper nanoparticles: A micro-structural and antibacterial activity investigation. J. Saudi Chem. Soc. **21**, 180–118 (2017)
12. M. Navid Rabiee, M. Bagherzadeh, A.M. Kiani, F. Ghadiri, A.H. Etessamifar, A. Jaberizadeh, Shakeri, (2020), Biosynthesis of Copper Oxide Nanoparticles with Potential Biomedical Applications, International Journal of Nanomedicine, 2020: 3983–3999
13. N. Cioffi, L. Torsi, N. Ditaranto et al., Copper nanoparticle/polymer composites with antifungal and bacteriostatic properties. Chem. Mater. **17**(21), 5255–5262 (2005). doi:10.1021/cm0505244
14. K. Anju Arya, T.S. Gupta, Chundawat, D. Vay, (2018), Biogenic Synthesis of Copper and Silver Nanoparticles Using Green Alga Botryococcus braunii and Its Antimicrobial Activity, Bioinorgaic Chemistry and Application, 2018: 7879403
15. I. Sarah, M.M. Bukhari, H. Hamed, Mohamed, H.S.S. Al-Agamy, H.H. Gazwi, Radwan, A.M. Youssif, (2020). Biosynthesis of Copper Oxide Nanoparticles Using Streptomyces MHM38 and Its Biological Applications, Journal of Nanomaterials, 2020: 6693302
16. S. Dipali Nagaonkar, M.R. Shende, Biosynthesis of copper nanoparticles and its effect on actively dividing cells of mitosis in Allium cepa. Biotechnol. Prog **31**(2), 557–565 (2015)
17. D.P. Chattopadhyay, B.H. Patel Preparation characterization and stabilization of nano sized copper particles Int. J. Pure Sci. Technol. **9**(1), 1–8 (2012)
18. Nabil Bouazizi, Ahmida El achari, Christine Campagne, Julien Vieillard, and A. Azzouz (2018). Copper oxide coated polyester fabrics with enhanced catalytic properties towards the reduction of 4-nitrophenol, Journal of Materials Science: Materials in Electronics, 29: 10802–10813
19. P.A. Golnaz Taghavi, F. Dary, F. Yirij, J.Cobley Lath, KrishnanaAndrew, Functionalised copper nanoparticle catalysts for electroless copper plating on textiles. Surf. Coat. Technol. **396**, 125971 (2020)

20. E. Auyeung, W. Morris, J.E. Mondloch, J.T. Hupp, O.K. Farha, C.A. Mirkin, J. (2015). Controlling Structure and Porosity in Catalytic Nanoparticle Superlattices with DNA, Am. Chem. Soc., 2015, 137, 1658–1662
21. Z. Hou, Effects of Cu, N, and Li intercalation on the structural stability and electronic structure of cubic Cu 3N. Solid State Sci. **10**(11), 1651–1657 (2008)
22. A.B.D. Nandiyanto*, R. Oktiani, Risti Ragadhita How to Read and Interpret FTIR Spectroscope of Organic Material Indonesian Journal of Science & TechnologyIndonesian Journal of Science & Technology,Volume 4 Issue 1, 4 (1) (20April19)2019 97 – 1 18Page 97–118

Figures

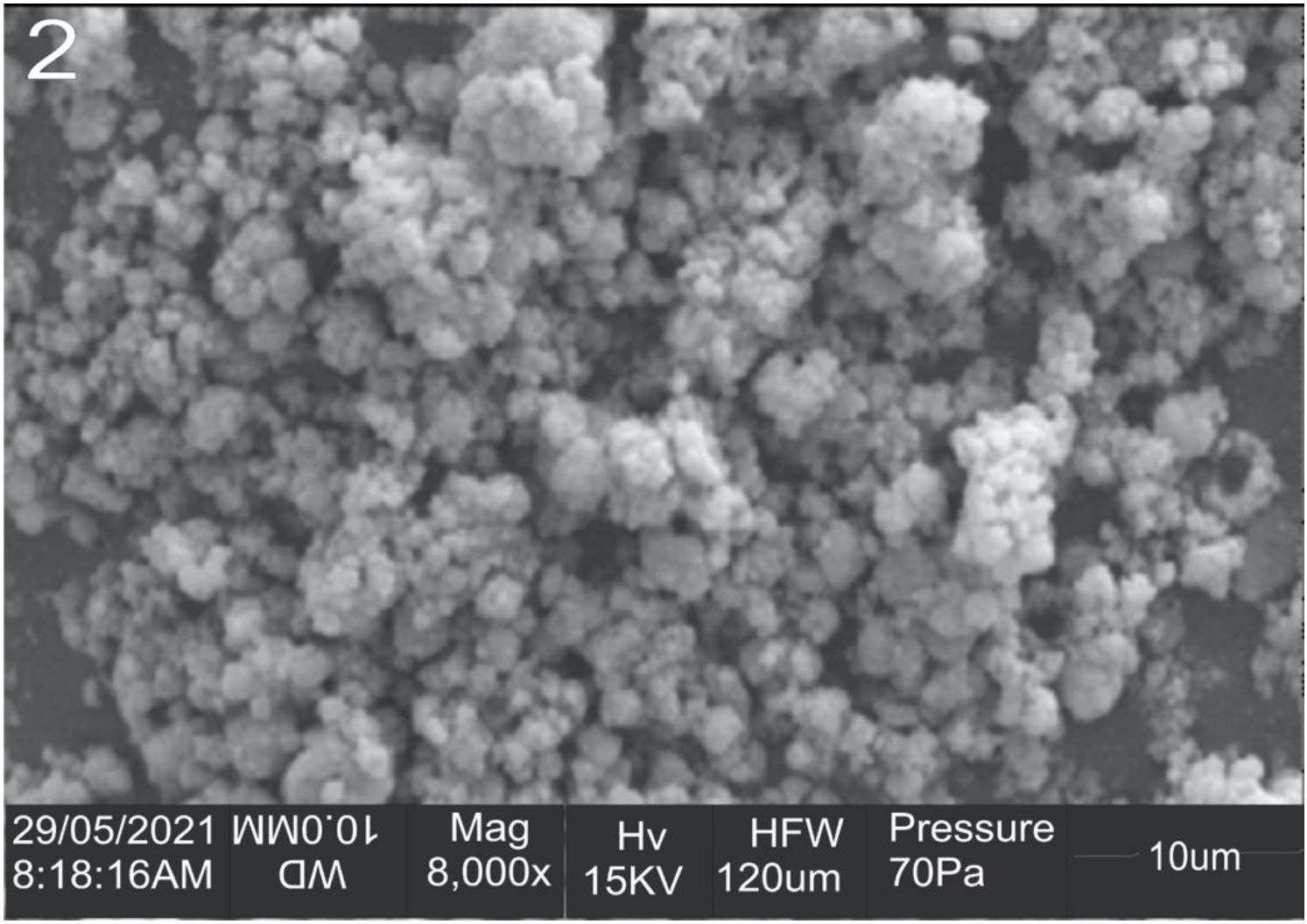

Figure 1

Morphology analysis of Cu-NP from leave extract

Figure 2

Morphology analysis of Cu-NP from bark extract

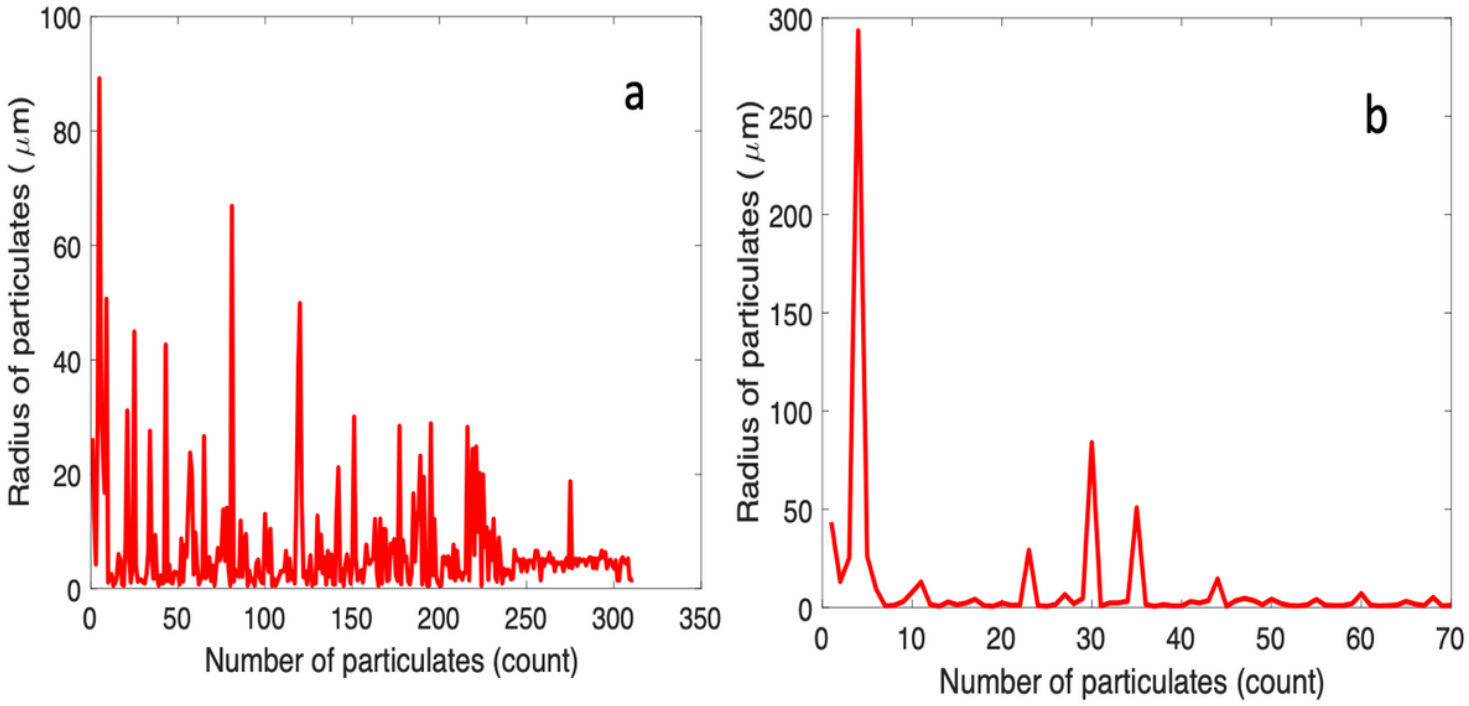

Figure 3

Particle size distribution (a) Cu-NP from leave extract (b) Cu-NP from bark extract

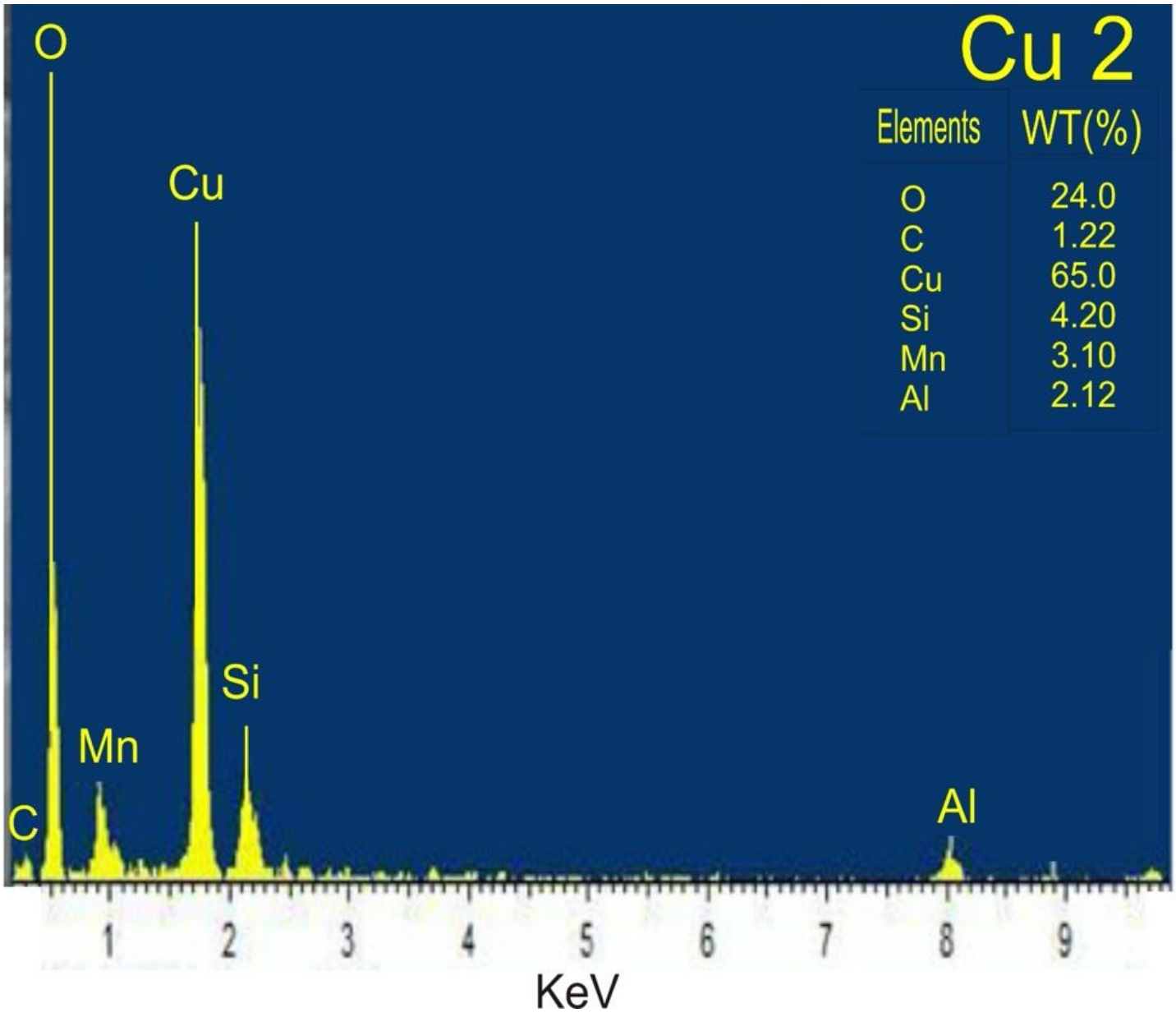

Figure 4

Compositional analysis of Cu-NP from bark extract

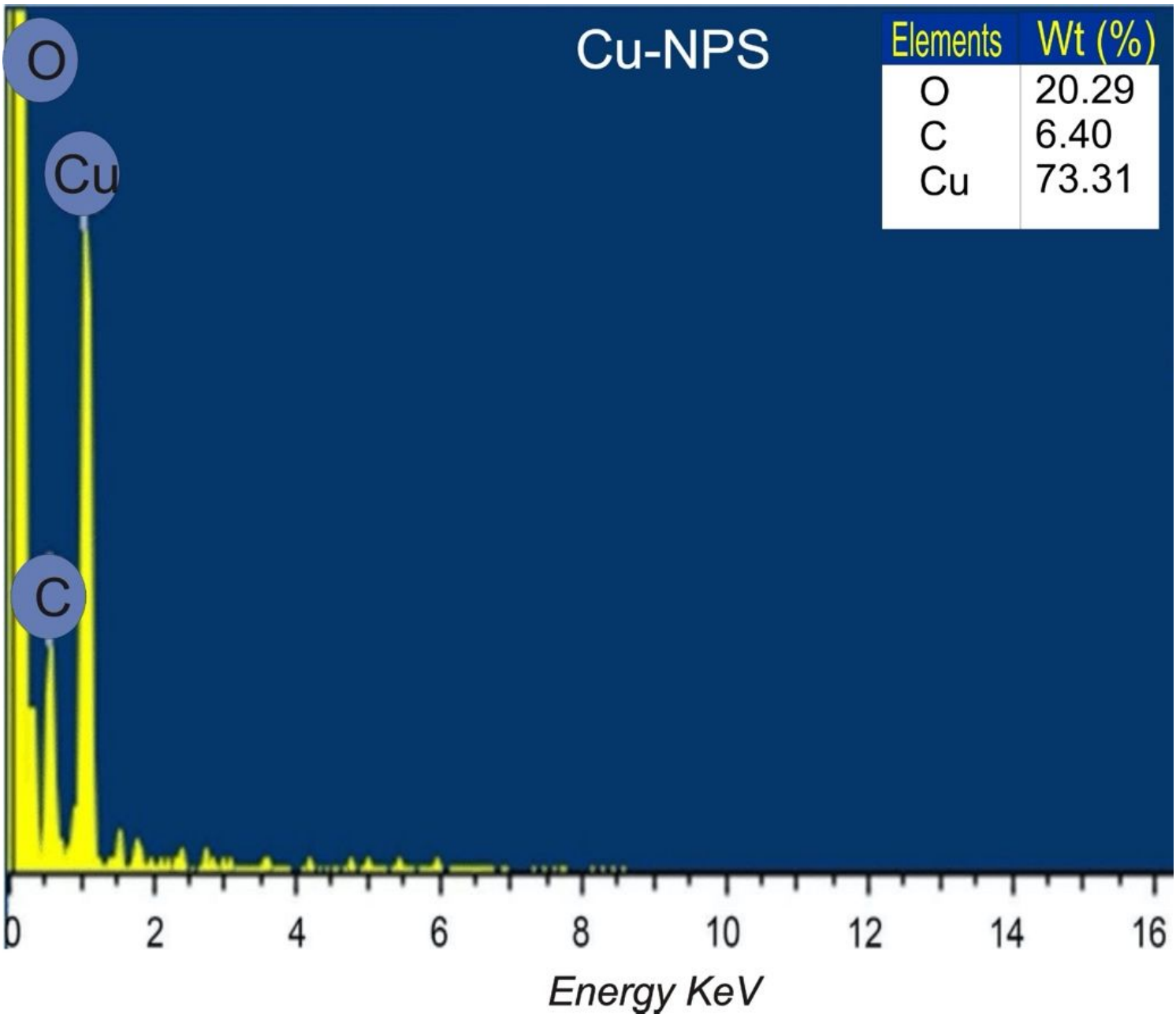

Figure 5

Compositional analysis of Cu-NP from leave extract

Figure 6

Crystallinity of Cu-NP in leave extract

Figure 7

Crystallinity of Cu-NP in leave extract

Figure 8

Functional group analysis of Cu-NP from bark extract

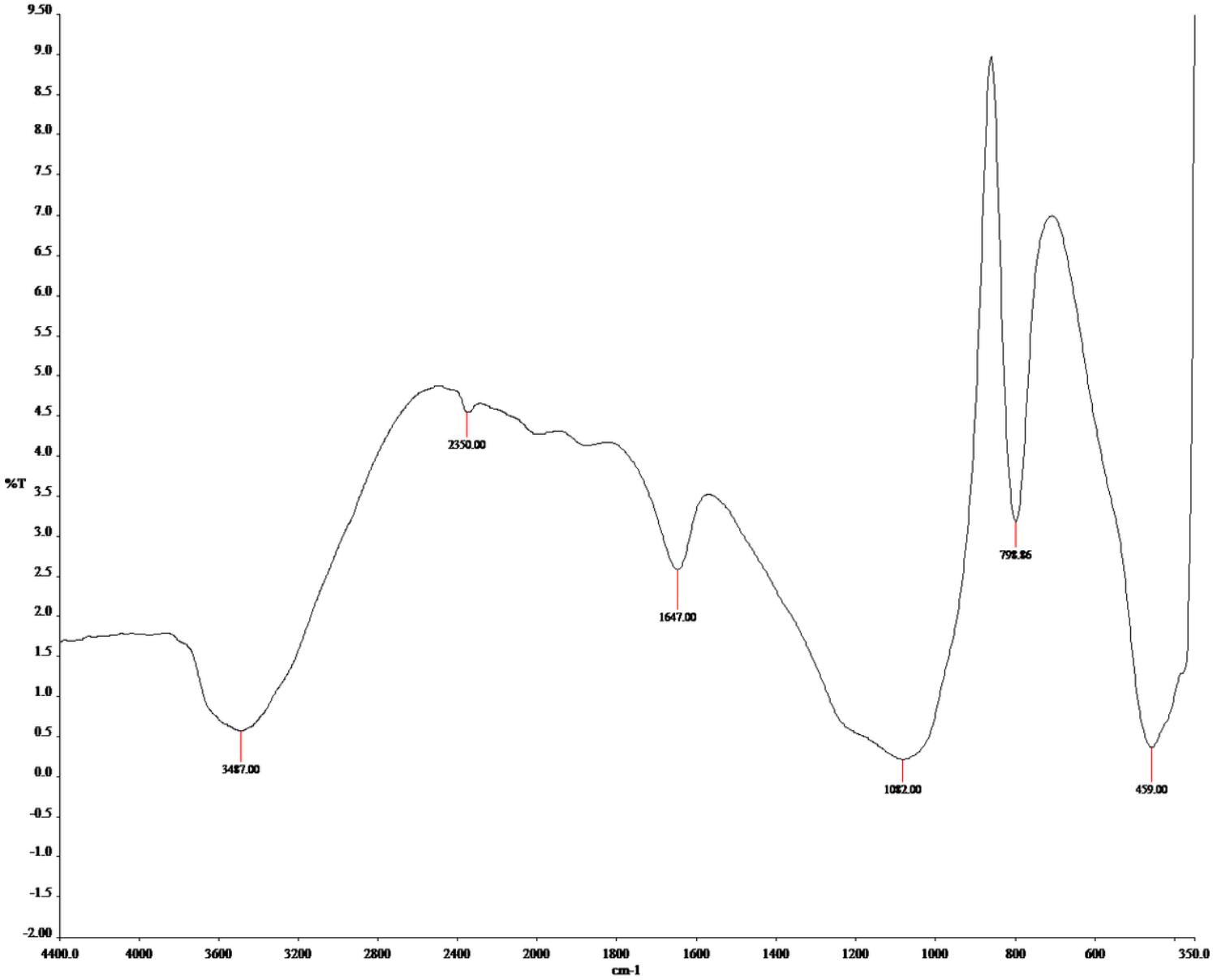

Figure 9

Functional group analysis of Cu-NP from leave extract